A Michelson Interferometer for Vibration Measurements, Fibre Noise Cancellation Setup, Study of Ion Trap Loading Mechanisms

Ana Sotirova

Technical reports on the work done as a summer student in the
Trapped Ion Quantum Information Group

ETH Zürich

Supervised by
Chiara Decaroli
Roland Matt
Robin Oswald
Prof Dr Jonathan Home

September 2018

Contents

Chapter 1

Michelson interferometer for vibration measurements

1.1 Experimental Setup

I am following the method described in Andrei Militaru's masters thesis. I am using a standard Michelson interferometer setup with one mirror attached to the target and the other - to a piezo crystal. The interference pattern is converted into voltage using a photo detector and the output signal is fed into a PI controller (EVIL). The output of the EVIL is then connected to the input of the piezo driver. If the signal fed into the PI is properly locked, then the output of the EVIL is proportional to the target vibrations. For more detailed theory see [1].

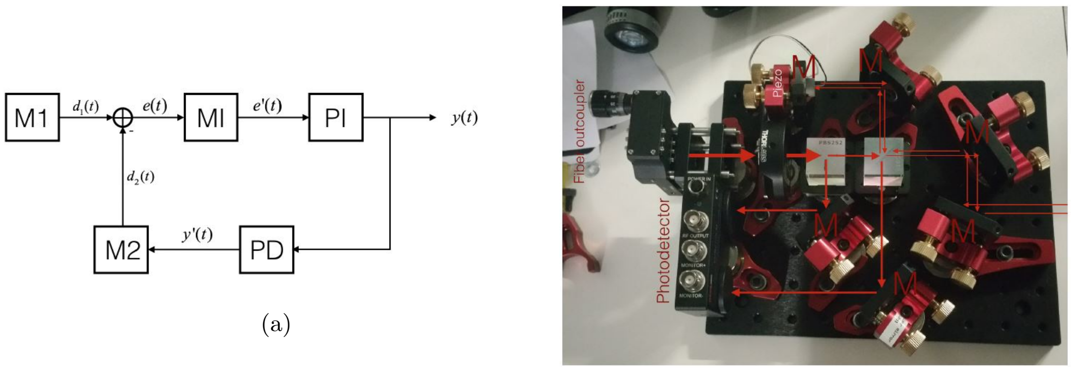

(a)

(b)

Figure 1.1: Experimental setup [1].

1.1.1 Alignment

The setup is built on a small breadboard and can easily be placed in front of the target mirror. I recommend using visible light at least for the alignment. As a first step make sure you are hitting the mirror on the target (and not e.g. the sides of the viewport). If this is the case the reflected point must be of roughly the same intensity as the one coming from the laser. Then overlap the incoming and the reflected beams. Finally at the photodetector the light coming from the target mirror and that coming from the piezo must also be well overlapped.

1.1.2 Checking the alignment

To check the alignment, connect the input of the piezo driver to a waveform generator and feed it with a triangular wave. Alternatively, you can use the Sweeping mode of the EVIL and then connect the output of the photodetector and the voltage monitor of the piezo driver to an oscilloscope so that you can observe both signals simultaneously. You should be able to see a few fringes as shown in Figure 1.2.

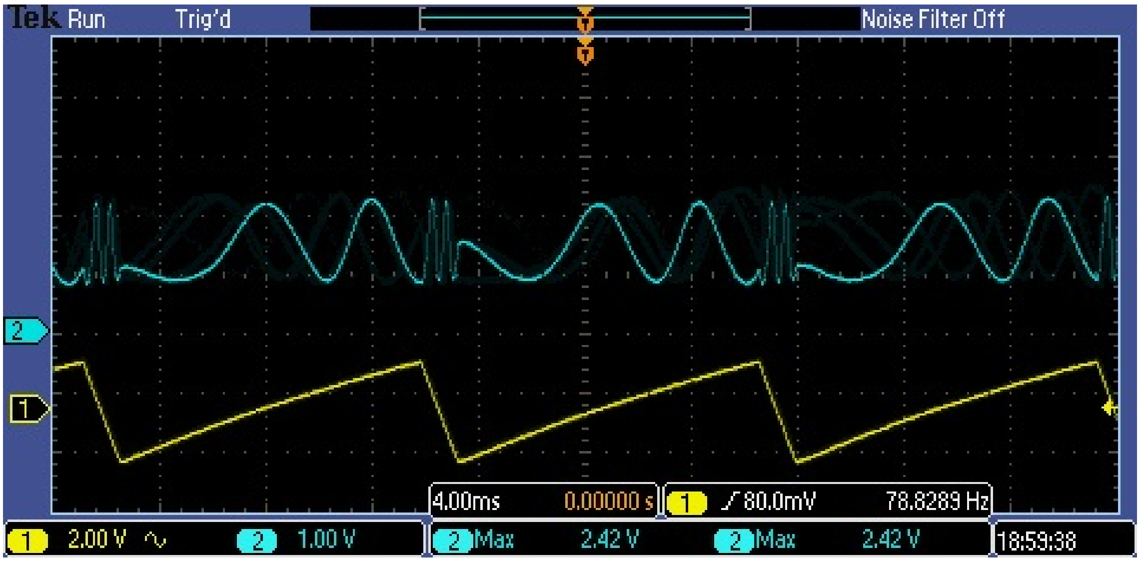

Figure 1.2: EVIL Ramp Output (yellow) and signal form photodiode (blue).

NB If you are using a signal generator make sure that the offset is set so that there is no negative voltage given to the piezo.

1.2 Measurements

Once the interferometer is working correctly and a nice interference can be observed, you can try to measure the vibrations of the target. For this purpose, take an EVIL (a PID controller). Then:

1. Connect the FOut (SOut) output of the EVIL to the input of the piezo driver.
2. Connect the output of the photodetector (either RF or Monitor -) to input A (B) of the EVIL.
3. Open the DEVIL (Dashboard for EVIL) GUI (installation instructions can be found on the wiki page). With a small screwdriver adjust the gain and the offset potentiometers on the EVIL until you see a signal of amplitude of about 100 on the GUI centered roughly at 0.
4. Start by sweeping with appropriate center, range and frequency such that the piezo driver does not overload and you can see the whole ramp nicely. You should be able to observe at least one fringe.
5. The signal locks to the horizontal yellow line. It should be roughly at the center of the signal (it can be moved by adjusting the input offset setting on the DEVIL). Adjust the P and I gains until the error signal looks reasonably flat and locked. Start by adjusting the I gain first. It is safe to use a high I gain, however care must be taken when setting the P gain.
6. To observe the signal given to the piezo connect the VoltageMonitor of the piezo driver to a scope. The data can then be extracted and analysed.

NB When the EVIL jumps to a new fringe, the signal may seize to be locked for a moment and the piezo might overload. Sometimes it goes back to normal on its own. If not, go to sweeping mode, adjust the input offset if necessary and then go back to controlling mode. You should be able to lock for at least 10-20 s so that enough data can be collected from the scope.

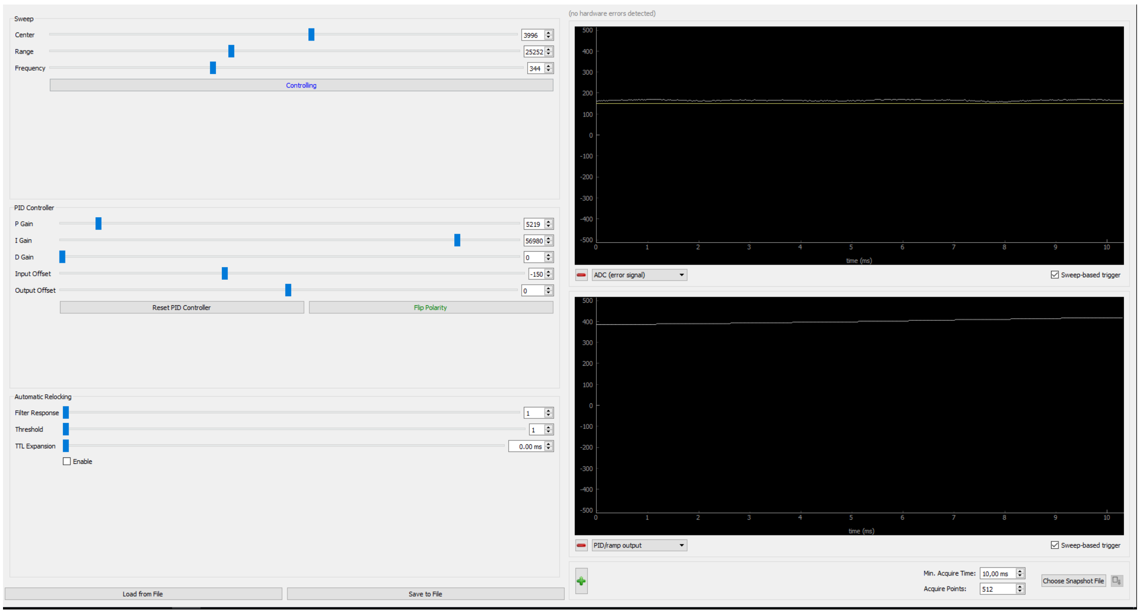

Figure 1.3: Example EVIL settings used for locking.

1.3 Analysis

1.3.1 Voltage to displacement conversion

The data extracted from the scope gives the time dependence on the voltage given to the piezo driver. As we are interested in the displacement of the mirror, we need to figure out a way of converting between the two. For that purpose we can estimate the total displacement of the piezo corresponding to a given change of the voltage. To do that, take a waveform generator and use it to drive the piezo, while observing the interference pattern on the scope. For example, in Figure 1.4 we see that there are 3 fringes corresponding to a voltage change of 6.7 V. The wavelength used is 729 nm. Suppose that the separation between the two mirrors is Δx. Then the OPL difference of light hitting the mirrors is $2\Delta x$ which corresponds to a phase difference $\delta = 2k\Delta x$ where k is the wavenumber given by $k = \frac{2\pi}{\lambda}$. Then the observed amplitude is

$$u = u_0(1 + e^{2ik\Delta x}) = 2u_0 e^{ik\delta x} \cos(k\Delta x) \tag{1.1}$$

which corresponds to observed intensity

$$I \propto 4u_0^2 \cos^2(k\Delta x) = 2u_0^2(1 + \cos(2k\Delta x)) \tag{1.2}$$

This has a maximum when $2k\Delta x = 2n\pi$ for some integer n, i.e. when $\Delta x = \frac{n\lambda}{2}$, and a minimum when $2k\Delta x = (2m+1)\pi$ for some integer m, i.e. when $\Delta x = (m + \frac{1}{2})\frac{\lambda}{2}$. Thus, the distance that the mirror on the piezo travels in order to get from a maximum to a minimum in the intensity is $\frac{\lambda}{4}$. Thus the three fringes in Fig. 4 correspond to a total displacement of the mirror

$$\Delta x = \frac{3\lambda}{2} = 1093.5\ nm \tag{1.3}$$

Assuming linearity, this gives a conversion factor

$$c = \frac{\Delta x}{\Delta V} = 163\ nm/V \tag{1.4}$$

Finally, taking into account the gain of the piezo driver g = 20 gives an overall conversion factor of m = c/20 = 8.15 nm/V.

1.3.2 Frequency domain

By using the conversion factor from the previous section we can deduce the time dependence of the displacement. To convert the data to the frequency domain, take the Fourier transform of the

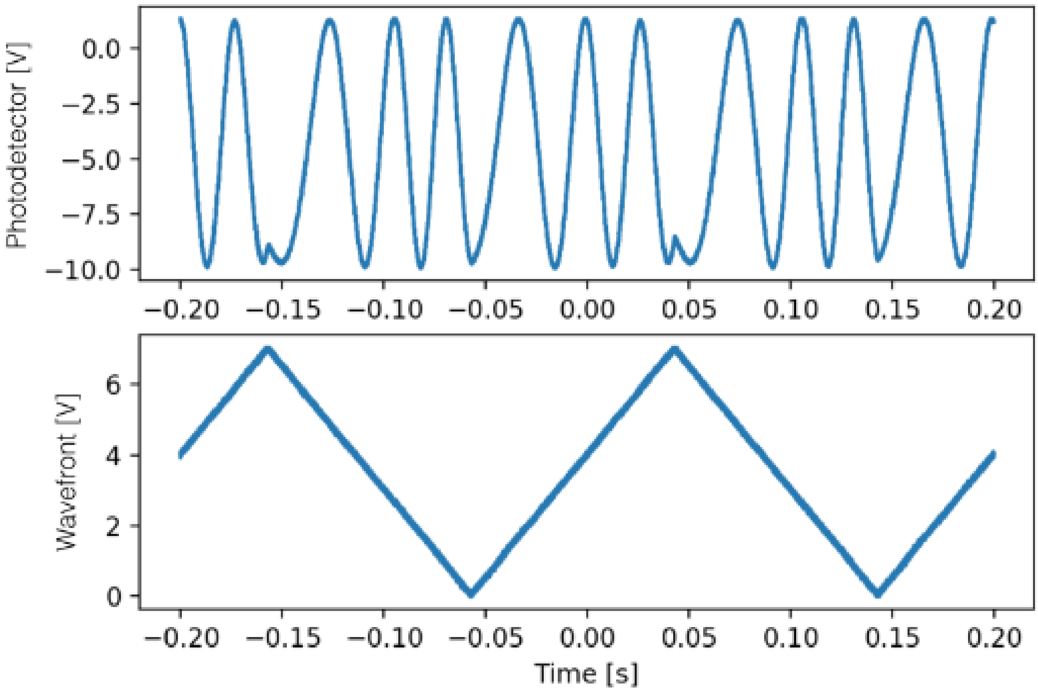

Figure 1.4: Photodetector output and signal given to the piezo used for estimating the conversion factor [1].

array defined (in 1D) as:

$$\tilde{f}(\omega) = \int f(t)e^{-i\omega t}dt \tag{1.5}$$

Now consider a signal which is a superposition of sinusoids of different frequencies:

$$f(t) = \sum_i V_i \sin(\omega_i t) = Im(\sum_i V_i e^{\omega_i t}) \tag{1.6}$$

The Fourier transform of this signal is given by:

$$\tilde{f}(\omega) = \int (\sum_i V_i e^{\omega_i t})e^{-i\omega t}dt \tag{1.7}$$

$$\tilde{f}(\omega) = \sum_i V_i \int e^{(\omega_i - \omega)t}dt \tag{1.8}$$

$$\tilde{f}(\omega) = \sum_i V_i \delta(\omega_i - \omega) \tag{1.9}$$

Hence, in the idealised case, the Fourier transform of the signal will consist of sharp peaks at the frequencies of the various sinusoids with amplitudes, equal to the original amplitudes of the sinusoids.

There are a couple of considerations to be taken into account when taking the Fourier transform of actual data. First, in the example above I considered a continuous signal. Real measuring instruments have finite sampling time, hence the eventual signal that can be read off is discrete. One problem which arises in this case is that of aliasing.This means that the highest frequency component that can be measured is limited by the sampling frequency of the apparatus used according to the Nyquist-Shannon sampling theorem [3]. Thus if you want to go up to a frequency of, say, 1 kHz, you need a sampling frequency of at least 2 kHz corresponding to 0.5 ms sampling interval.

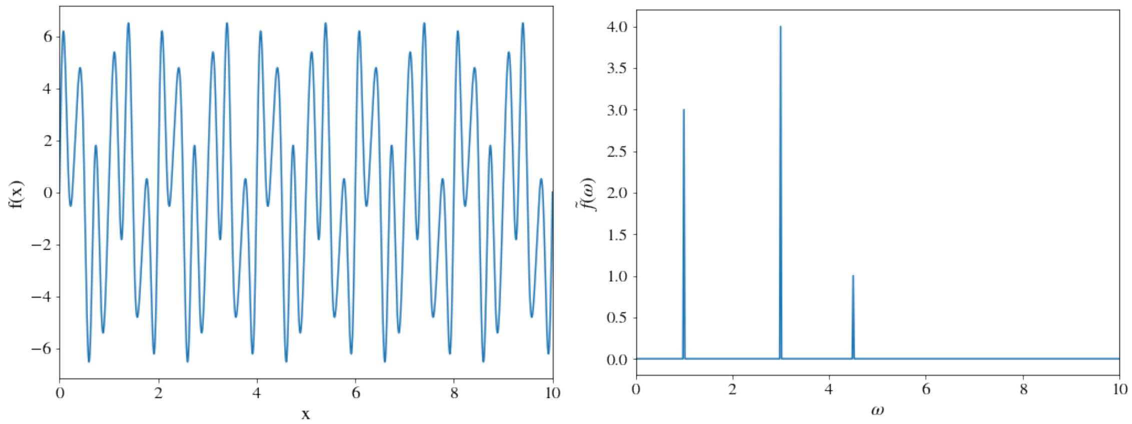

(a) (b)

Figure 1.5: Fourier transform of dummy data. (a) $f(x) = 3sin(2\pi x) + 4sin(6\pi x) + sin(9\pi x)$. (b) Fourier transform of f(x).

A final consideration is which plot to use. There are two options - amplitude vs frequency or power spectral density (PSD) vs frequency. The PSD contains information about the power content of the signal [4]. It is important when characterising broadband random signals when an amplitude vs frequency plot is not so reliable. However, here this is not the case and hence I recommend using an amplitude vs frequency plot as the magnitude of the vibrations can be directly read off from it.

1.4 Example measurements

A couple of measurements were performed on Roland and Robin's trap with the cryostat on and off. The root-mean-square displacement when the cryostat was on was measured to be 40 nm. Further factor to be taken into account is electrical cords being plugged into the chamber as they will carry the vibrations of any external apparatus (including the cryostat).

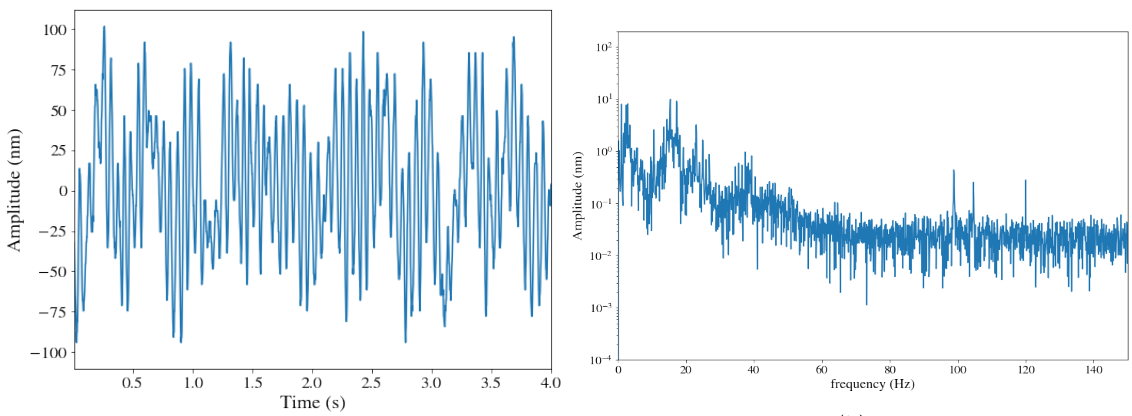

(a) (b)

Figure 1.6: Vibration measurement results with the cryostat on.

Chapter 2

Fibre noise cancellation setup

2.1 Introduction

A wide range of atomic physics experiments rely on using laser light to drive transitions between atomic states thus making long coherence time and narrow linewidth crucial characteristics of the laser source and the optical fibre used as a transmission medium. These can be significantly impaired by phase noise written onto the fibre by the laser or by pressure and temperature variations in the lab. The finite linewidth of a single-frequency laser can easily be narrowed down to a Hz-level by locking it to a high-finesse cavity. Phase noise due to acoustic fluctuations in the lab is more dangerous as it can raise the output linewidth to a kHz-level. This technical report gives a theoretical background on phase noise and methods of cancellation, and explains how to use the fibre noise cancellation (FNC) setup in the isolated black box in B18.

2.2 Theoretical Background

2.2.1 Phase noise

Phase noise refers to random rapid oscillations of the phase of a waveform. A light wave propagating through a given medium can be described by an electric field given by:

$$\mathbf{E} = E_0 cos(\omega t + \phi(t)) \tag{2.1}$$

If we assume that the initial phase is 0, ϕ will depend on the optical path travelled by light:

$$OPL = \int_{\gamma} n(r) ds \tag{2.2}$$

In the presence of acoustic noise the OPL, and hence the phase, will be time-dependent and $\phi(t)$ will describe the phase noise written onto the fibre. The fibre response is reasonably flat in the 100Hz-2kHz regime [5], so the spectrum of the phase noise will primarily depend on the acoustic noise spectrum in the environment. To cancel optical phase noise, the phase $\phi(t)$ is first measured and then a phase $-\phi(t)$ is written onto the fibre prior to transmission using an AOM. To see how this can be achieved, consider two light waves generating photocurrent amplitudes i_A and i_B, phases ϕ_A and ϕ_B and frequency difference ω_Δ being overlapped on a photodiode [6]. The mean induced photocurrent is then given by:

$$i = i_A + i_B + 2\sqrt{i_A i_B} cos(\omega_\Delta t + (\phi_A - \phi_B)) \tag{2.3}$$

Now assume that $\omega_\Delta = 0$ and that $\phi_{A,B} << 1$ and let $\phi_A = 2\phi_\epsilon$ and $\phi_B = -2\phi_{AOM}$. Then the above expression gives:

$$i \propto cos(2\phi_\epsilon + 2\phi_{AOM}) \approx 2\phi_\epsilon + 2\phi_{AOM} \tag{2.4}$$

This is used as an error signal which vanishes when $\phi_\epsilon = \phi_{AOM}$, i.e. when the phase of the AOM matches the phase acquired by light during transit through the fibre.

2.2.2 Acousto-optic modulators

An acousto-optic modulator (AOM) is a device which uses acoustic waves to modulate the frequency, intensity and/or the direction of the incoming light [7]. When a sound wave travels through a crystal it induces regions of higher and lower refractive indices. As a result, light incident on the crystal scatters and interferes. To see this, consider an acoustic wave of wavelength Λ travelling in the positive z-direction through a crystal lying between two infinite planes at y=0 and y=d. Consider also a plane monochromatic light wave of wavelength λ incident on the crystal (Figure 2.1). When light enters the crystal it will scatter due to stratifications in the material produced by the sound wave and we will observe regions of constructive and destructive interference. From diffraction theory we know that in order to observe constructive interference, the optical path difference between the interfering rays must be an integer multiple of the wavelength of light λ. From Figure 2.1 this condition is equivalent to:

$$AD - BC = \Lambda(\sin\phi_2 - \sin\theta_2) = n\lambda \tag{2.5}$$

for some integer n. By using Snell's law

$$\frac{\sin\theta_1}{\sin\theta_2} = \frac{\sin\phi_1}{\sin\phi_2} \tag{2.6}$$

we can rewrite (2) as

$$\Lambda(\sin\phi_1 - \sin\theta_1) = n\lambda \tag{2.7}$$

Thus the angular separation between consecutive orders can be written as

$$\Delta\phi = \frac{\lambda}{\Lambda} \tag{2.8}$$

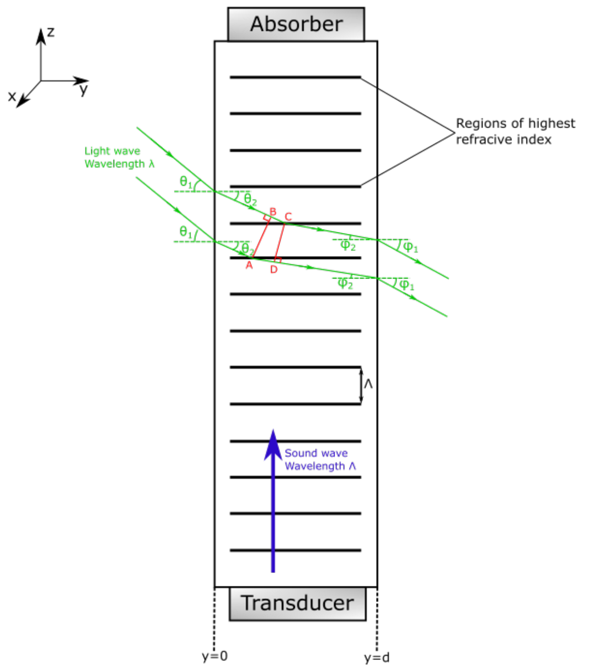

Figure 2.1: Principle of operation of an AOM.The transducer generates acoustic waves travelling trough the crystal. To avoid the formation of a standing wave an absorber is added on the other end of the crystal.

From (8) we see that the angular separation of neighbouring orders decreases as Λ increases. Thus, in order to be able to observe a diffraction pattern, a small wavelength (i.e. a large frequency) of the acoustic wave needs to be used. In most setups the AOMs are driven with a frequency of the order of a few hundred MHz.

To understand the change in frequency, we can think of the process as photons colliding with phonons. In that case conservation of energy for the collision between a photon and m phonons gives

$$h\Delta f = mE_{phonon} \tag{2.9}$$

$$\Delta f = \frac{mE_{phonon}}{h} \tag{2.10}$$

If m>0 then m photons are absorbed during the collision and the frequency of light increases. On the other hand, if m<0 then m phonons are created during the collision and the frequency of light increases.

The main challenge when working with AOMs is to be able to distinguish between the 1^{st} and the -1^{st} order. This is determined by the direction of propagation of the acoustic wave. The first order is always in the same direction from the zeroth order, as the direction of propagation of the acoustic wave (Figure 2.2). In practice, to determine the zeroth order, move the mirror screws until no diffraction is observed and you can see only a single spot - this is the zeroth order. Then the first order is found trivially.

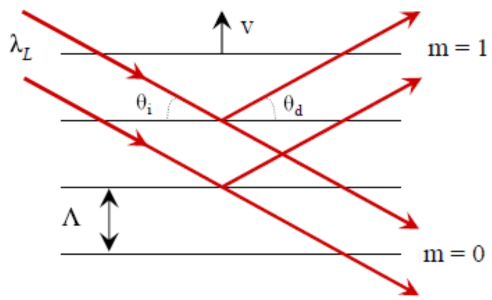

Figure 2.2: Bragg construction for identifying diffraction orders from an AOM [8].

The AOM is usually controlled via an AOM driver which consists of a voltage controlled oscillator (VCO), a voltage variable attenuator (VVA), and an amplifier. The VCO uses a reference voltage to control the frequency of the sound wave driving the AOM. A second voltage supplied to the VVA controls the degree of the attenuation and finally, the VVA output is amplified, so that the final RF wave is sufficient to drive the AOM. Such a circuit is employed in the POISON board (see section 5.1).

2.3 Experimental setup

The full experimental setup is shown in Figure 2.3 and Figure 2.4. It consists of an optics and an electronics part. The optical setup works as follows. Light from the laser is diffracted by an AOM and the 0^{th} order is retroreflected using a mirror. The first order is coupled into a fibre and a small fraction of the light (about 4%) is retroreflected by a window right after the outcoupler. The retroreflected light is then passed back through the AOM and the two beams are overlapped. The beat frequency of the two beams carries the phase difference $2\phi_{AOM} - 2\phi_{\epsilon}$ (1) and can be measured using a photodiode.

2.4 Black box

The setup is made of two levels (Figure 2.5). Level I is slightly larger than level II due to height constraint from the isolation box. We use 30 cm rods from stranda (now eksma) to connect the two levels. The bottom level hosts the HF cavity, which will be left in its position, together with the optics required for it. Everything else will be moved to accomodate the rods. There are two different posts height used in the setup: tall posts (Radiant Dyes), which are already used for the

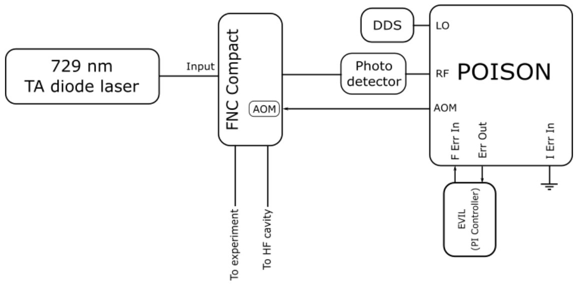

Figure 2.3: Overview of the experimental setup. For full description of the FNC Compact see section 4.1 and Figure 2.6. For the POISON board see section 2.5.1 and appendix A.

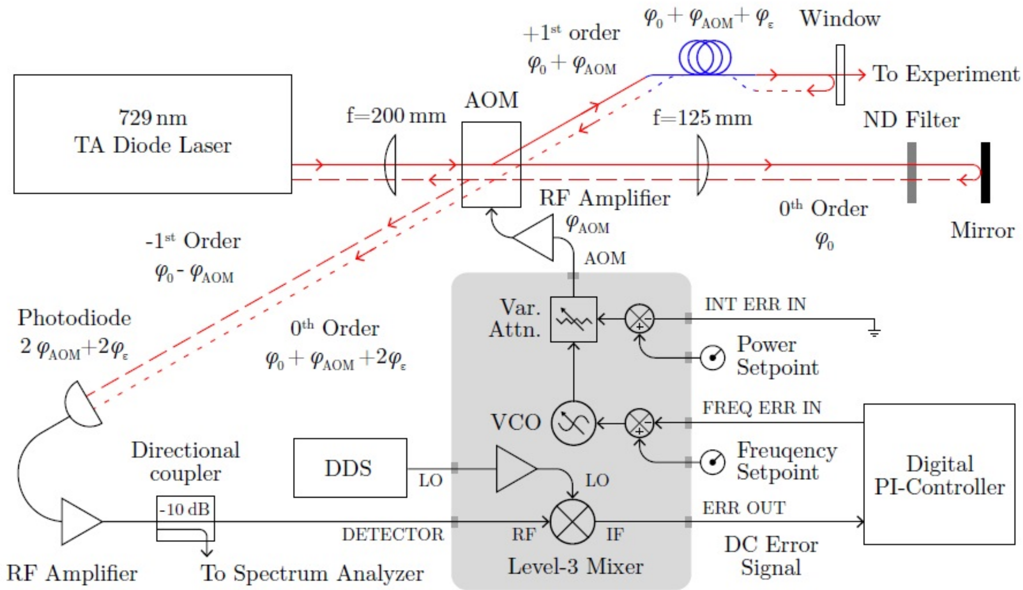

Figure 2.4: Full experimental setup [6].

cavity optics and have a resulting beam height of 125 mm, and small mounts (Thorlabs Polaris) directly attached to the optical table which have a beam height of 12.446 mm. Polaris mounts are screwed on custom aluminium breadboard of 10 mm thickness, therefore the beam height for compact fnc setups is of 22.446 mm with respect to the bigger optical breadboard. Table stable legs model AVI 200 M are used to provide stability to the whole setup. These legs need to be calibrated according to the weight they carry. A height separation of 30 cm also allows easy manipulation and alignment of the optics on the lower level. To bring the light to the upper level, we design a custom periscope attached to both breadboards. We then create a side pocket on the upper breadboard to easily insert the periscope. We choose a periscope over a fibre due to the fact that the TA will have the highest efficiency for the full injected light, and using a fibre to link the two would introduce losses. In the following sections, we will describe the theory of injection, fibre noise cancellation and light amplification, and present the designs of the modular setups which can be replicated with little effort. We hope to provide guidance in future optical setups designs.

2.4.1 FNC Compact

There are 4 such boards in the black box - one on level 1 and three on level 2. Note that the boards on level 2 do not have Path 1. Start aligning the optics by choosing a suitable position of the PBS such that the light hits the middle of the mirrors on the two sides of it. Then coupling into the fibre going to the HF cavity should be relatively trivial and the usual tricks apply (e.g. using a fibre pen to match the two spots, walking the beam, etc.).

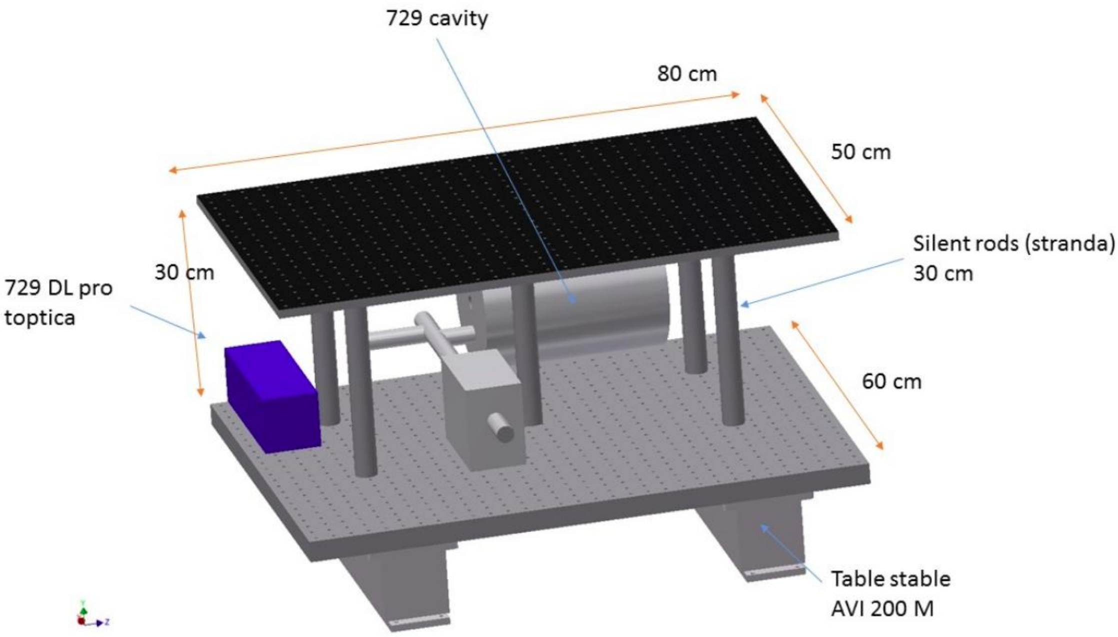

Figure 2.5: Black box setup.

For the path with the AOM:

- Use the bottom mirror on the left to make the beam go as close as possible to the centre of the bottom lens. Then move the lens so that the beam going through is reasonably focused and you see a nice round spot. Use the next mirror to make sure you are hitting the active area of the AOM.
- Switch on the AOM and observe the diffracted pattern. Use the bottom left and bottom right mirrors to get to the optimal horizontal and vertical position of the beam so that the diffraction pattern is of greatest intensity. You can further try to increase the intensity by walking the beam using the same two mirrors. You might also need to tilt the AOM.
  NB Remember to make sure you are seeing a 0^{th} and 1^{st} order (rather than -1^{st}). In the current setup the 1^{st} order is to the right of the 0^{th}. To check move the beam up or down a bit until you lose the diffraction pattern and see a single spot - this is the 0^{th} order.
  Finally, adjust the horizontal position slightly so that most of the power is going in the 1^{st} order.
- Next, place the lens so that both the 0^{th} and the 1^{st} order are passing through. The 0^{th} order should go to the mirror directly behind the lens and then be reflected to the mirror to the very right of the board. Using the last two remaining mirrors couple the 1^{st} order into the fibre going to the lab. For this use a fibre pen and first overlap the spot from it with the 1^{st} order directly in front of the AOM. Then it should be relatively easy to get light coming out of the fibre and optimise the intensity by walking the beam. Since the 1^{st} order will usually be elliptical, it will be hard to achieve coupling efficiency of more than 20-25%.
- Now there will be two reflected beams to work with - one from the tip of the fibre going to the lab and the other - from the rightmost mirror. The reflected 0^{th} order will be diffracted again when passing through the AOM. Overlap the 1^{st} diffracted order with the reflected spot from the fibre and make sure they hit the photo diode nicely so that the induced photo current can be measured.

2.4.2 Injection

Optical injection locking is a mechanism by which a "master" laser at a specific frequency is locked to a high power laser diode, the "slave", in order to produce high power light at the master frequency. As lasers are mechanical oscillators, one can intuitively magine coupling two oscillators at

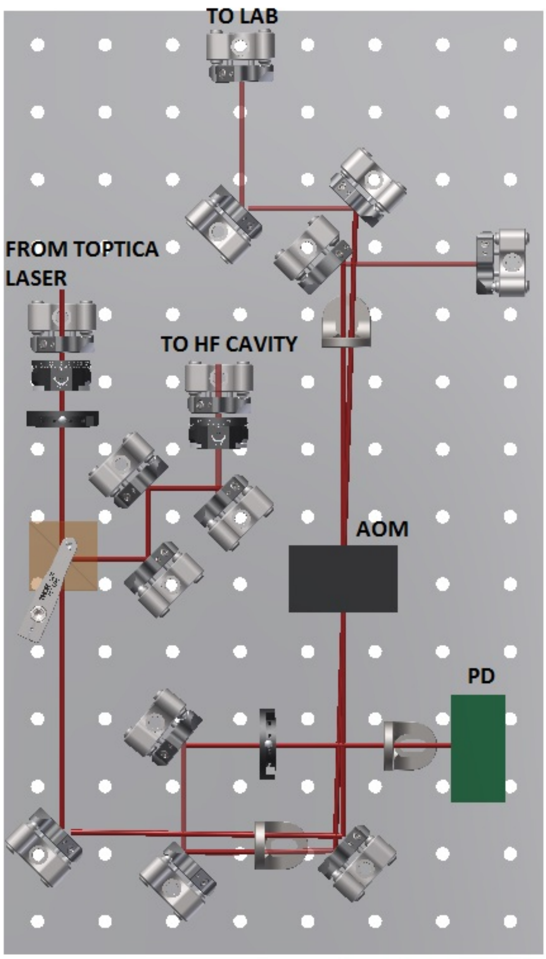

Figure 2.6: FNC compact setup.

different frequencies. In this coupled system, the "master" will start to force the "slave" to oscillate at its own frequency. Injection is used as a way to amplify an optical signal while maintaining its spectral purity. In our setup, we are recycling some light transmitted through a high finesse cavity. As this light is a very weak power light source, we need to inject it with a diode before we can use it to seed a Tapered Amplifier (TA). Clean injection is achieved when only light at the master source frequency is the output of the injection. This situation can be achieved by tuning three parameters: the temperature of the diode, the current driving the diode and the intensity of the diode. The first two parameters modify the refractive index of the diode cavity, and as a result vary the modes supported by the cavity. The third parameter is important as the output intensity depends on intensity of the diode, and of the injected light.

We use a commercial diode (model:) to inject the trasmitted light from the HF cavity. The power of the master is:. Injection depends on the square root of the ratio between of the diode laser power and the master laser power and the decay rate of the diode cavity.

2.4.3 Periscope design

We use a custom design for the periscope in order to have a stable support and to be able to deliver light at the required height. The beam height contraint fixes the total height of the periscope mount to 375 mm. We create an inlet in the upper breadboard in order to slide the periscope easily from the side. We fix the periscope on both the lower and upper breadboard using small legs which can be clamped using usual optical forks.

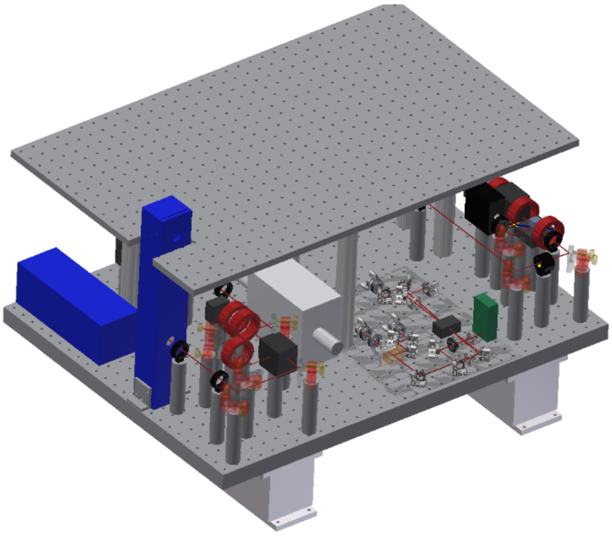

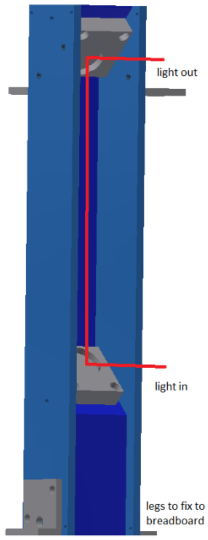

Figure 2.7: Full setup.

2.5 Electronics

2.5.1 POISON

The POISON boards consists of two independent ciruits. One of the ciruits is used to drive a voltage controlled oscillator (VCO) with appropriate offset and frequency, and the other detects the phase error given by (4).

VCO circuit

The voltage source circuit consists of two low-noise variable circuits used for tuning the VCO voltage and the variable RF attenuator. The corresponding channels are DETECTOR, LO, ERR OUT. The first stage of this circuit is a low-noise 2.5 V voltage reference U1. The voltage of U1 is controlled by the 10 kΩ potentiometer V1. Make sure that the voltage on the voltage reference does not exceed the specified value of 2.5 V, otherwise it burns out and needs to be changed. The next stage is an operational amplifier U2 in an inverting configuration and gain of $-R3/(VR2 + R2)$. The input voltage of the op-amp is controlled by adjusting the 10 kΩ potentiometer VR2. U2 also contains a second op-amp which is used as a buffer and also inverts the result. This part of the board is used for controlling the frequency of the output with VR1 providing the rough adjustment and VR2 being used for fine tuning. There is a completely analogous circuit right after the variable RF attenuator with corresponding voltage reference and amplifier U11 and U12 and potentiometers VR11 and VR12. This part of the board is used for adjusting the amplitude of the signal.

Phase detector circuit

The phase detector circuit consists of a frequency mixer, a direct digital synthesizer (DDS) and an amplifier. The frequency mixer mixes the photodiode signal to DC and the DDS acts as a stable frequency reference with a kHz-level phase noise. Finally, the op-amp buffers the IF voltage and filters fast-frequency components from the error signal.

Testing the board

Before switching on the boards make sure that VR1 and VR11 are turned fully counterclockwise. Otherwise the voltage on the voltage references will be too high and they will overload.

1. **Testing the VCO**
    - Terminate all channels except for AOM and connect the AOM to a scope.

- Power up the board. You can use a rack, although during first tests using a triple power supply is desirable, as it will enable direct access to the elements. If using a triple power supply, set it to ±15 V and connect GND to pin 1, -VCC to pin 30 and +VCC to pin 31 of the Eurocard connector. Set the current limits to about 200 mA. The typical current drawn is 150-200 mA from the positive terminal and about 25 mA from the negative terminal.
- As a first step make sure that the signal observed on the scope responds to adjusting of the potentiometers VR1, VR2, VR11, VR12. VR1 and VR2 should change the frequency, and VR11 and VR12 should change the amplitude. Again, make sure that while tuning VR1 and VR11 the voltages on pin 6 of U1 and U11 remain below 2.5 V.
- If the above step works, then probably this part of the testing is OK. However, if you want to be sure, use VR2 to fine tune the output frequency. Then measure the voltage on Pin 5 of the VCO and the frequency of the signal and compare them with the ones in Table 1.

Output frequency (MHz)	**VCO Pin 5 voltage (V)**
147.5	1.54
156.0	2.03
162.3	2.5
167.2	2.8
170.6	3.1

Table 2.1: VCO circuit testing data.

2. **Testing the frequency mixer**

- Get an RF signal generator and connect it to the LO channel.
- Connect AOM (VCO output) to the DETECTOR channel.
- Connect F ERR Out to a scope.
- If you want to be very safe, terminate F/I Err In.
- Measure the frequency of the AOM output (can be done beforehand during testing the VCO or by using pin 10 of the voltage attenuator).
- Set the frequency of the RF generator to be 1-2 MHz away from the frequency of the VCO output. Otherwise, you will hit the bandwidth of the U101 op-amp and the signal output from F Err Out will be severely attenuated (and you might even see no signal at all).
- The frequency of the output signal should then be equal to difference of the frequencies of the signals going in LO and GENERATOR.
- Example data is given in Table 2.

AOM peak-to-peak voltage	500 mV
AOM frequency	123.5 MHz
RF generator frequency	120 MHz
Mixer pin 2 pp voltage	220 mV
F Err Out pp voltage	180 mV
F Err Out frequency	3.5 MHz

Table 2.2: Frequency mixer circuit testing data.

Troubleshooting

The most common source of problems is adjusting U1 and/or U11 such that the voltage on the voltage references is more than 2.5 V. This usually results in the voltage references having to be replaced. However, sometimes this might lead to problems with the op-amps as well.

- If there is a problem with the voltage references, then the voltage drop on Pin 6 will not change as the potentiometers VR1/VR11 are adjusted.
- If the voltage references work OK, but the signal on the scope does not react to tuning the potentiometers, check the voltage on R5/R15. If the voltage drop on R5/R15 is not 0, then most likely the op-amps need to be changed.

Display boards

The display boards have 22 LEDs of which 11 are for monitoring the VCO voltage and 11 are for monitoring the RF variable attenuator voltage. Whenever the supplied voltages are too high, some of the LEDs will light up. In that case, use the potentiometers to adjust the voltages until no LED is on. Note that potentiometers VR1 and VR11 are for rough adjustment and need to be set before placing the display boards. The only potentiometers we have access to once the whole board is built and placed in a box are VR2 and VR12 which are for fine adjustment only.

Chapter 3

Ion trap loading mechanisms

3.1 Introduction

Nowadays various areas of physics make use of ion traps. The following report presents a brief description on the four most common ion trap loading mechanisms and discusses their advantages and disadvantages. The main factors taken into account are reliability, reproducibility, contamination of the trap electrodes, expected loading time, and isotope selectivity.

3.2 Atomic oven

Atomic ovens are by far the most commonly used source of atoms. They work by means of resistively heating up a sample covered with the desired material. As a result, the material evaporates or sublimates and a cloud of hot atoms is produced. The atoms can then be cooled to energy suitable for trapping by using resonant photoionisation. This method of ion loading is not isotope selective, so if more than one species is required, a separate oven will need to be built for each element. The main advantage of atomic ovens is their ability to be mounted on vacuum-compatible PCBs. However, care must be taken to prevent contamination of the trap surfaces and shorting of the trap electrodes due to metal deposition. A further complication arises when using the technique in cryogenic environment due to temperature rises during the loading process. The heating process will reach a steady state due to thermal energy dissipation. Typical required oven temperatures for Ca and Be ovens are: 433° for Ca, corresponding to a current of 2.7 A and 790° for Be corresponding to a current of 1.4 A [11]. Subsequent photoionisation is most effective when the electron energies are a few times the ionisation potential of the element[12]. Thus, after the ion is trapped, we need a few seconds until it is cool enough to produce a reliable signal. Usually resisitively heated ovens take 2 to 5 minutes to heat up enough from room temperature. This limits the rate of data acquisition and if the oven is left on, the rise in background pressure will impair the trap lifetime. The Oxford group built a resistively heated atom sourse which requires just 12 s preparation time [13].

3.3 Magneto-optical trap (MOT)

3.3.1 Principle of operation

If an atom is moving in the presence of a laser beam it will experience a radiative force. Now consider an atom in the presence of two low-intensity laser beams propagating in opposite directions. If the beams have the same intensity and frequency, the net radiative force on a stationary atom will vanish. However, if the atom is moving along the path of the light, and the laser is tuned below resonance, the frequencies of the two beams will be Doppler shifted. Light co-propagating with the atom will be shifted closer to resonance and light anti-propagating will be shifted away from resonance. Hence, the atom will interact more strongly with light in the opposite direction and its velocity will decrease. For small velocities, the net force can be approximated to be proportional to the velocity of the atom, hence the situation is analogous to viscous damping. If we use three orthogonal pairs of laser beams confinement of atoms in a very small volume in all three directions

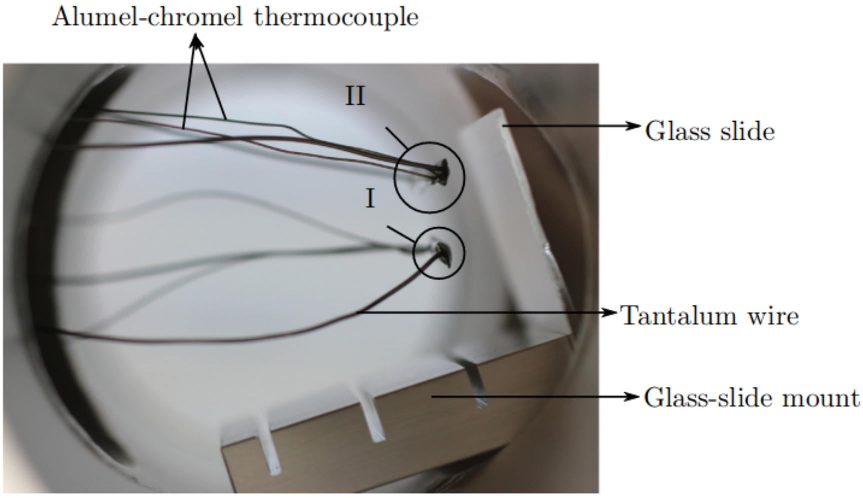

Figure 3.1: Caclium oven setup used in the TIQI group [11].

can be provided. Further a quadrupole magnetic field is added to the setup such that as the atom moves away from the origin, the transition is Zeeman shifted (see section 4.1) and it is pushed back by one of the beams. For more detailed theory see page 156 of [14].

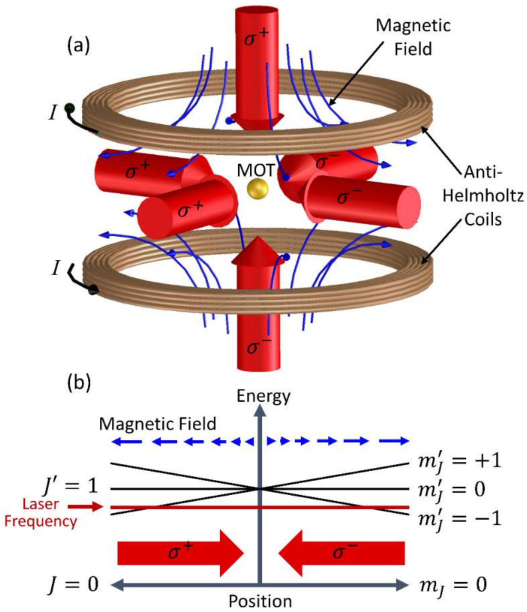

Figure 3.2: Principle of operation of a magneto-optical trap [15]. (a) MOT setup. (b) Energy diagram along one direction of the MOT.

3.3.2 Advantages and disadvantages

Without a doubt, this technique offers better isotope selectivity over the other conventional ion trap loading mechanisms. This is due to the fact that the MOT is intrinsically isotope-selective. Furthermore, in some experiments the atomic oven used to load atoms in the MOT has no line of sight with the trapping region and a push beam is used to move the cold atoms to the trap. This further improves the isotope selectivity and also prevents contamination of the trap electrodes. Compatibility of the technique in a low-temperature environment (4.6 K) has also been demonstrated [16].

3.4 Zeeman slower

3.4.1 The Zeeman effect

The Zeeman effect describes the effect of a magnetic field on atoms. Suppose that we have a particle with angular momentum $\mathbf{L}$ and spin-angular momentum $\mathbf{S}$ in a magnetic field described by the vector potential $\mathbf{A}$. Then the Hamiltonian of the particle can be written as

$$H = \frac{1}{2m}(\mathbf{p} \;-\; q\mathbf{A})^2 \;+\; V(r) \tag{3.1}$$

Now let's assume that the applied magnetic field is weak (compared to the spin-orbit interaction) so that when expanding the above expression we can neglect quadratic terms in the magnetic potential. This gives

$$H \approx H_0 - \frac{q}{m}\mathbf{p}\cdot\mathbf{A} \tag{3.2}$$

where $H_0 \;=\; \frac{p^2}{2m} \;+\; V(r)$ is the original Hamiltonian of the system. Over the size of the atom we can approximate the magnetic field to be constant, so we can assume that the magnetic potential can be chosen to be

$$\mathbf{A} \;=\; \frac{1}{2}\mathbf{B}\times\mathbf{r} \tag{3.3}$$

Then the Hamiltonian becomes

$$H \;=\; H_0 - \frac{q}{2m}\mathbf{p}\cdot(\mathbf{B}\times\mathbf{r}) \;=\; H_0 - \frac{q}{2m}\mathbf{B}\cdot(\mathbf{r}\times\mathbf{p}) \;=\; H_0 - \frac{\mu_B}{\hbar}\mathbf{L}\cdot\mathbf{B} \tag{3.4}$$

where the Bohr magneton is defined as $\mu_B = \frac{e\hbar}{2m}$. Hence the angular momentum magnetic moment of the electron can be written as

$$\mu_L = -\frac{\mu_B}{\hbar}\mathbf{L} \tag{3.5}$$

Further the spin magnetic moment for an electron is

$$\mu_S = -\frac{\mu_B}{\hbar}g_S\mathbf{S} = -2\frac{\mu_B}{\hbar}\mathbf{S} \tag{3.6}$$

giving a total magnetic dipole moment

$$\mu = -\frac{\mu_b}{\hbar}(\mathbf{L}+2\mathbf{S}) \tag{3.7}$$

and a perturbing Hamiltonian

$$\delta H = -\mu\cdot\mathbf{B} = \frac{\mu_B}{\hbar}(\mathbf{L}+2\mathbf{S})\cdot\mathbf{B} \tag{3.8}$$

Then the first-order energy shift computed in the $|j, m_j, l, s\rangle$ basis is

$$\delta E = \frac{\mu_B}{\hbar}B\,\langle j, m_j, l, s|\,(L_z + 2S_z)\,|j, m_j, l, s\rangle = m_j\mu_B B\left[1 + \frac{j(j+1) - l(l+1) + s(s+1)}{2j(j+1)}\right] \tag{3.9}$$

Thus the Zeeman effect splits the degenerate energy levels in an atom proportionally to the applied magnetic field. Such an energy splitting gives rise to pairs of lines in emission spectra, allows for determining the quantum numbers of an atom and is used in atom cooling devices such as the Zeeman slower. For more details see [17].

3.4.2 The Zeeman slower

The Zeeman slower makes use of the Zeeman effect to cool atoms from room temperature to a few Kelvins. The atoms are cooled by using a pump laser pointed in a direction opposite to their motion and a spatially varying magnetic field. The pump laser is tuned a bit away from resonance. Initially it slows down a particular velocity class of atoms via Doppler cooling. As the beam passes through the device the resonant frequencies of other velocity classes are Zeeman shifted allowing for the laser to become resonant with them and slow them down via Doppler cooling as well. Usually a magnetic field along the z-axis is chosen such that the atoms experience a constant acceleration. It can be shown[18] that the required form of the magnetic field is

$$B(z) = B_0 + B_\alpha \sqrt{1 - \frac{z}{z_0}} \tag{3.10}$$

3.4.3 Advantages and disadvantages

Just like the MOT, this method is intrinsically isotope-selective. The Zeeman slower is extremely useful if the temperature required by the oven is very high and it is not efficient to load the atoms directly into a MOT. Thus, in such setups the Zeeman slower is put between the oven and the MOT to cool the atoms prior to entering the MOT.

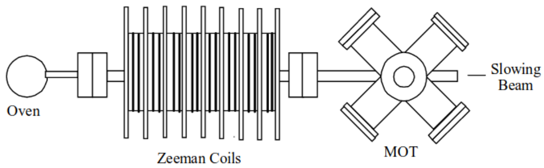

Figure 3.3: An example use of a Zeeman slower [19].

3.5 Laser ablation loading

3.5.1 Characteristics of the process

Laser ablation is the process of removing a material from the surface of a given solid or liquid by focusing a laser beam onto it. The success of the ablation process depends on the following factors:

- **Wavelength** The appropriate wavelength to use is determined by the type of material in use. If the penetration depth of the material for the given wavelength is small, there will be a large amount of energy deposited into a small volume resulting in better efficiency of the process.
- **Beam quality** We are mainly interested in the spot size and the focus ability of the beam. Better focus and a narrower spot allow for maximum laser intensity to be present on the target and the illumination of the surrounding surface to be minimised.
- **Pulse duration and pulse repetition rate** Short pulse duration is desirable as this allows for maximum peak power and lowest illumination of the surrounding surface. Furthermore, laser ablation heats up the surface so a high pulse repetition rate is desirable as in this way the surface doesn't have time to cool down, less energy is lost and the process happens more quickly.

3.5.2 Advantages and Disadvantages

In its application to ion traps, laser ablation has the great advantage of very short loading time of the order of a few miliseconds[21]. It also avoids heating up the UHV chamber. Furthermore, creating a plume of neutral atoms requires much less effort than other loading mechanisms. The atoms can then be ionized by using either electron impact or resonant photoionization. However, laser ablation is not suitable for all systems. The atomic vapour produced as a result of the ablation process often contains not only the desired atoms, but also molecular ions of a variety of species and isotopes. This and the high kinetic energy of the products severely limits the loading efficiency and requires frequent recalibration of the electrode voltages for successful trapping. Using resonant photoionisation will increase the efficiency and will allow for better selectivity but will not completely avoid trapping other charged products.

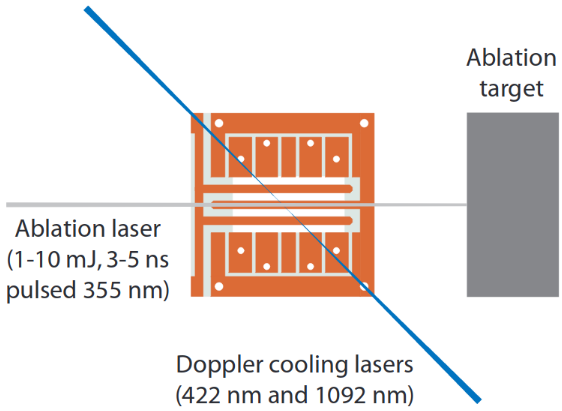

Figure 3.4: Use of ablation in loading a surface ion trap [20].

3.6 Summary

Method	Advantages	Disadvantages
Atomic oven	• easy to manufacture • vacuum compatible	• not isotope selective • danger of trap contamination and shorts • not suitable for cryogenic environments • slow loading time (2 to 5 minutes)
MOT	• isotope selective • prevents contamination of the trap • compatibility with cryogenic environment	• sometimes a push beam is needed • requires more space; usually placed outside cryostat
Zeeman slower	• isotope selective • useful if oven temperature is about 1000 K	• needs a MOT afterwards to furher cool down the atoms
Laser ablation	• short loading time (a few miliseconds) • it doesn't heat up the UHV chamber • easier to create a plume of neutral atoms than other mechanisms	• not isotope selective • high KE of the products • requires frequent recalibration

Appendix A

Poison schematics

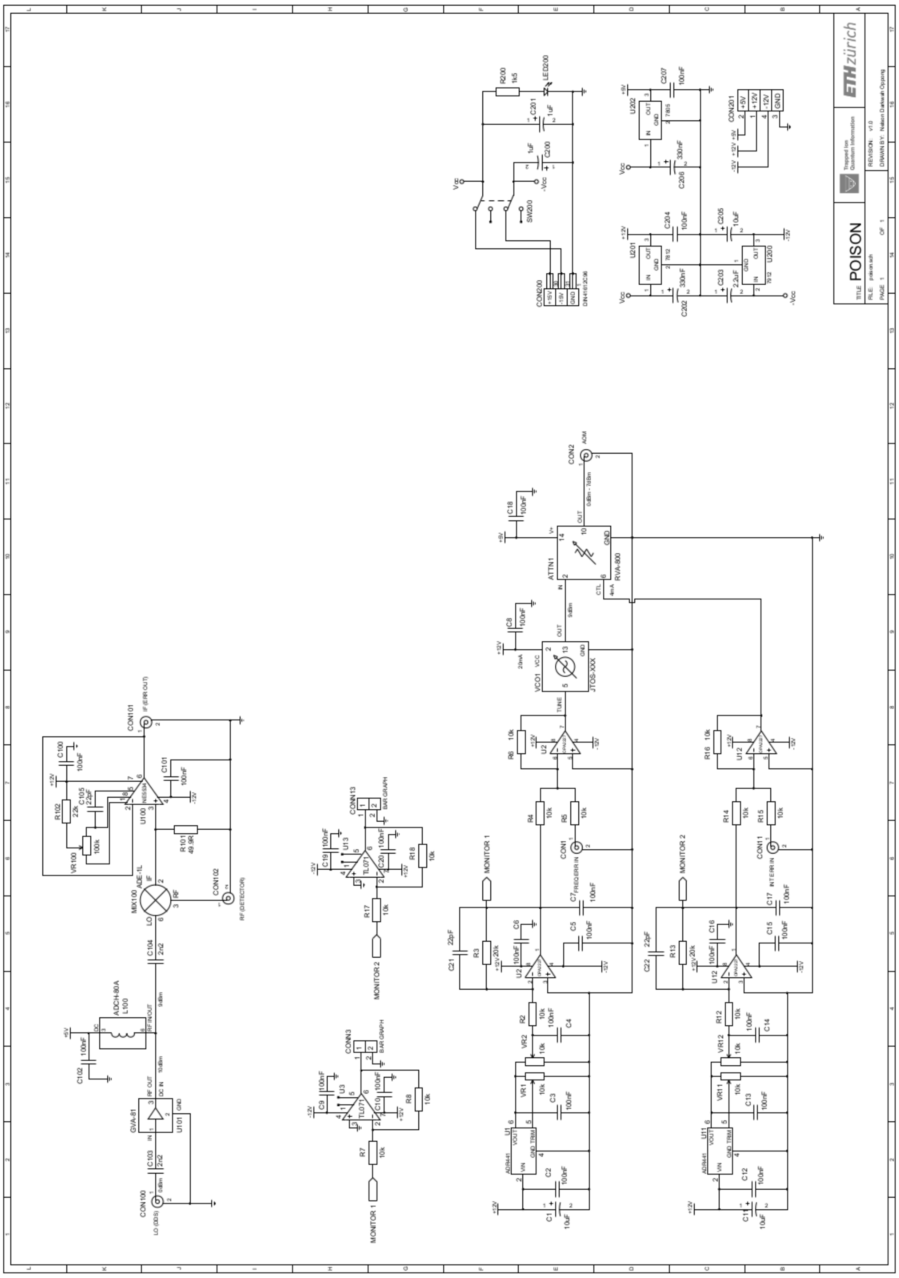

Figure A.1: POISON schematic [5].

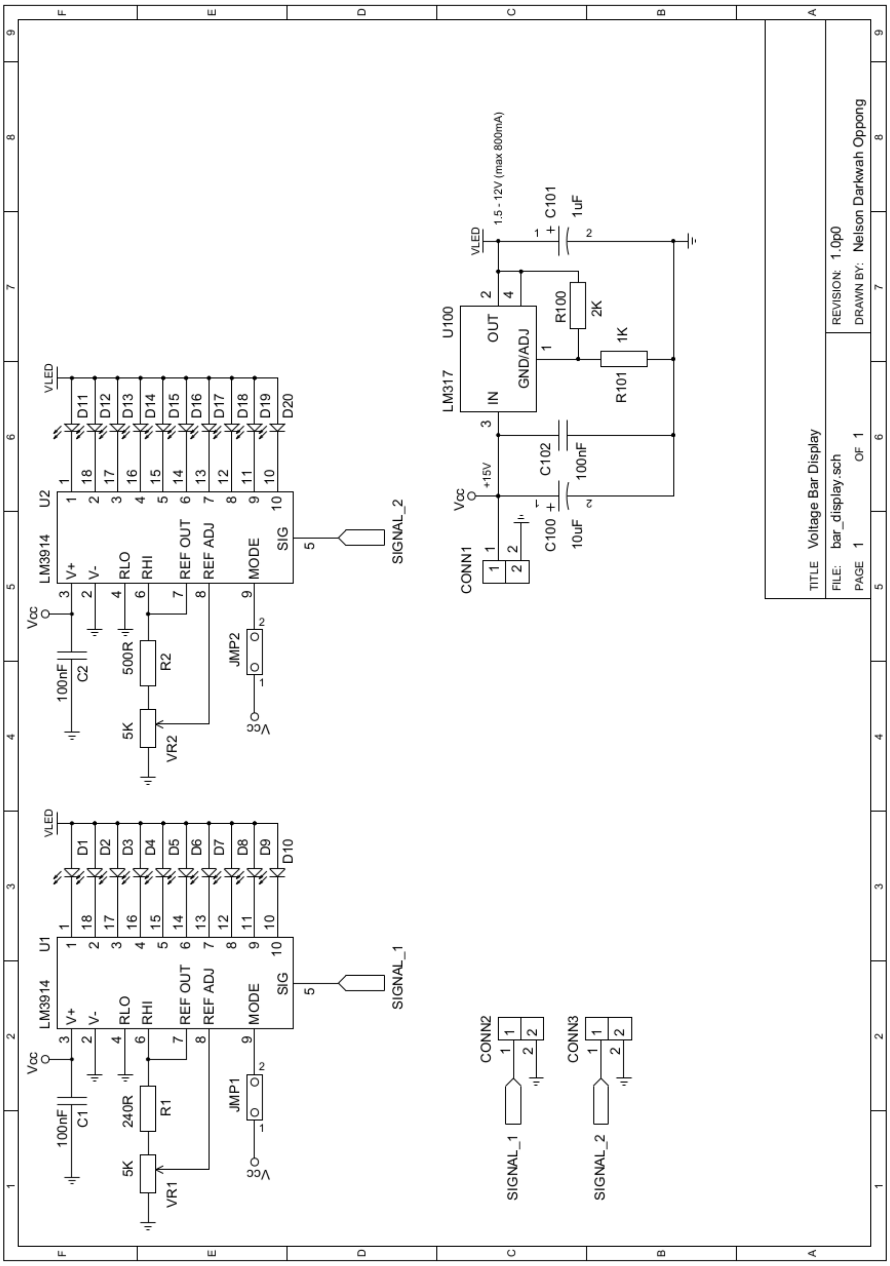

Figure A.2: POISON display board [5].

Bibliography

[1] Andrei Militaru, *"An Optical Setup for Single Ion Addressing in a Cryogenic Surface-Electrode Ion Trap"*, Masters Thesis, TIQI, ETH Zurich

[2] Max Born, Emil Wolf. *Principles of Optics*. Cambridge University Press, ISBN-13: 978-0-521-64222-4

[3] https://en.wikipedia.org/wiki/Nyquist-Shannon_sampling_theorem

[4] https://community.plm.automation.siemens.com/t5/Testing-Knowledge-Base/What-is-a-Power-Spectral-Density-PSD/ta-p/360969

[5] L.-S. Ma et al. "Accurate cancellation (to milliHertz levels) of optical phase noise due to vibration or insertion phase in fiber transmitted light". In: *Proceedings of SPIE* 2378 (1995), p. 165.

[6] Nelson Darkwah Oppong, *"Cancelation of optical phase noise induced by an optical fiber"*, Semester Thesis, TIQI, ETH Zurich

[7] Max Born, Emil Wolf. *Principles of Optics*. Cambridge University Press, ISBN-13: 978-0-521-64222-4

[8] McCarron, D.J., 2007. *A guide to acousto-optic modulators.*

[9] Christa Flühmann, *"Stabilizing laser and magnetic fields for quantum information experiments"*, Masters Thesis, TIQI, ETH Zurich

[10] Martin Sepiol, *"Stabilization of a 729 nm laser to an ultra-high finesse reference cavity"*, Masters Thesis, TIQI, ETH Zurich

[11] Roland Hablützel, *"Novel Atom Sources and Ultra-fast Electronic Switches for Trapped-Ion Quantum-Information Experiments"*, Masters Thesis, TIQI, ETH Zurich

[12] J. D. Sankey, A.A. Madej, Appl. Phys. B 49, 69-72 (1989)

[13] Timothy G. Ballance, Joseph F. Goodwin, Bethan Nichol, Laurent J. Stephenson, Christopher J. Ballance, David M. Lucas, Review of Scientific Instruments 89, 053102 (2018)

[14] Harold J. Metcalf, Peter van der Straten, *Laser Cooling and Trapping*, Springer, 1999, ISBN 978-0-387-98728-6

[15] Mcclelland, Jabez and V. Steele, A and Knuffman, B and Twedt, Kevin and Schwarzkopf, A and Wilson, Truman, Applied Physics Review 3, 011302 (2016)

[16] J. M. Sage, A. J. Kerman, and J. Chiaverini, Phys. Rev. A 86, 013417

[17] David J. Griffiths, *Introduction to Quantum Mechanics*, Second edition, Pearson, ISBN 978-1-292-02408-0

[18] https://en.wikipedia.org/wiki/Zeeman_slower

[19] Margaret Lynn Harris, *Design and construction of an improved Zeeman slower*, Masters Thesis, Duke University

[20] David R. Leibrandt, Robert J. Clark, Jaroslaw Labaziewicz, Paul Antohi, Waseem Bakr, Kenneth R. Brown, and Isaac L. Chuang, Phys. Rev. A 76, 055403

[21] Peng Zhou, *"Motional State Control and Ablation Loading in a Cryogenic Surface-Electrode Trap"*, Masters Thesis, TIQI, ETH Zurich